PHYSICAL REVIEW B VOLUME 13, NUMBER 10 15 MAY 1976

Strain effect on the electronic density of states and dc conductivity of disordered binary alloys

Hsing-chow Hwang* and Arden Sher*
College of William and Mary, Williamsburg, Virginia 23185

Chris Gross
NASA-Langley Research Center, Hampton, Virginia 23365

(Received 21 July 1975)

A single-band model calculation is developed for the effect of strain on the temperature variation of the electronic density of states and the electrical conductivity of disordered binary alloys. Experimentally, strain has only a small effect on the temperature variation of the conductivity. Shifts in the Fermi level and distortions of the density of states under different strains are found from the calculations. The small change in the temperature variation of conductivity under strain is a result of competition between these two effects. Methods to extract physical parameters characterizing alloys from measurements of the strain and temperature variation of the resistivity are discussed. Suggestions are also made about materials-selection criteria for strain-gauge applications.

I. INTRODUCTION

The macroscopic electronic properties of alloys, such as the dc electrical conductivity, have been fruitful subjects for experiments. But the theoretical interpretation of these properties has lagged far behind the wealth of experimental information. It is especially important to develop a theory for the resistivity of concentrated alloys, because many of the experimental methods that helped the understanding of pure metals, e.g., cyclotron resonance, de Haas–van Alphen effect, etc., do not work at all in alloys. For disordered systems many physical properties can be related to the configuration-averaged Green's function. There was a long search for a method to calculate this average Green's function, and the coherent-potential approximation[1] has been found to provide a convenient and accurate approximation for it. Chen, Weisz, and Sher[2] (CWS) have performed a model calculation of the temperature dependence of the electronic density of states and the electrical conductivity of disordered binary alloys, based on Velicky's[3] coherent-potential-approximation solutions by introducing thermal disorder in the single-band model. They found that the effect of thermal disorder is to broaden and smear the static-alloy density of states. The electrical conductivity in weak scattering alloys always decreases with temperature. However, in the strong-scattering case, the temperature coefficient of conductivity can be negative, zero, or positive, depending on the location of the Fermi energy. Brouers and Brauwers[4] have extended the calculation to an $s-d$ two-band model that accounts for the general behavior of the temperature dependence of the electrical resistivity in concentrated transition-metal alloys.

In this paper we generalize Chen *et al.*'s work to include the effect of uniaxial strain on the temperature variation of the electronic density of states and the electrical conductivity of disordered concentrated binary alloys. Experimentally strain has a small but measurable effect on the conductivity, and our model calculations reproduce this general trend. We find that the major effect of the strain is to introduce an effective scattering strength $\delta_{\text{eff}} = \delta + s^A - s^B$, where s^A and s^B are the strain deformation energies of the A and B atoms, respectively.

II. MODEL

The simplest possible model electron Hamiltonian that includes substitutional impurities, thermal disorder, and strain deformation, is that of a single-band model,

$$H = H_0 + D + \Theta + S \;, \tag{1}$$

where

$$H_0 = \sum_{m,n}{}' |m\rangle h_{mn} \langle n| \tag{2}$$

represents the part of the Hamiltonian off diagonal in site indices, and the transfer integrals h_{mn} are assumed to be periodic and independent of alloying and lattice distortion;

$$D = \sum_n |n\rangle \epsilon_n \langle n| \tag{3}$$

represents the "static-disorder" Hamiltonian with ϵ_n either ϵ^A or ϵ^B, according to whether an A or B atom is on site n;

$$\Theta = \sum_n |n\rangle \theta_n \langle n| \tag{4}$$

is the electron-phonon interaction; and

$$S = \sum_n |n\rangle s_n \langle n| \tag{5}$$

is the strain deformation Hamiltonian due to an external force (see Appendix A). The phonon operator θ_n depends on which ion occupies site n and on the phonon energy, while the deformation operator s_n depends on which ion occupies site n and the strain deformation energy.

Following the method of CWS it is easy to show that the appropriate generalization of their Eq. (66) for the single-site self-energy Σ when the strain energy is included is

$$\langle\langle(\epsilon_n+\theta_n+s_n-\Sigma)/[1-(\epsilon_n+\theta_n+s_n-\Sigma)F]\rangle\rangle=0\ , \qquad (6)$$

where as usual $F(z)=\langle 0\,|\underline{G}(z)|\,0\rangle$ is the site-diagonal average Green's function, and the double average denotes averages over configurations and thermal lattice displacements.

In order to calculate the conductivity and density of states, a method to compute the averages in the self-energy equation, Eq. (6), is needed. This has been accomplished for the electron-phonon interaction in CWS's paper,[2] and our attention is now directed to its generalization to include the strain deformation of the alloy.

III. DISTRIBUTION FUNCTION

In the spirit of previous calculations that treat only random diagonal terms, we can incorporate all off-diagonal contributions from phonons and strains into the hopping integrals. Then following the usual practice of dropping lowest-order effects of strain and phonons on the electron effective mass, we neglect them. The remaining electron-phonon and strain terms do not conserve crystal momentum and are represented in our model [Eqs. (4) and (5)] by the local Hamiltonian

$$H_{\mathrm{epd}}=\Theta+S=\sum_n |n\rangle(\theta_n+s_n)\langle n|\ . \qquad (7)$$

The phonon average of any function $f(\theta_n+s_n)$ of the operators θ_n and s_n is

$$\langle f(\theta_n+s_n)\rangle_p=\mathrm{Tr}_{\mathrm{ph}}[\rho_{\mathrm{ph}}f(\theta_n+s_n)]\ , \qquad (8)$$

where

$$\rho_{\mathrm{ph}}=e^{-\beta H_{\mathrm{ph}}}[\mathrm{Tr}_{\mathrm{ph}}(e^{-\beta H_{\mathrm{ph}}})]^{-1}\ , \qquad (9)$$

and the trace is over all states of the lattice motion. H_{ph} is the Hamiltonian describing the atomic motion of the alloy in a given configuration and is defined by

$$H_{\mathrm{ph}}=\sum_{s=1}^{3N}\hbar\omega_s(\tfrac{1}{2}+b_s^\dagger b_s) \qquad (10)$$

in the harmonic approximation, where $b_s^\dagger$ and b_s are the creation and destruction operators for a phonon in the state with frequency ω_s.

The average $\langle f(\theta_n+s_n)\rangle_p$ can also be written in terms of the probability distribution $P_n(\eta)$ as

$$\langle f(\theta_n+s_n)\rangle_p=\int_{-\infty}^{\infty}d\eta\, f(\eta+s_n)P_n(\eta)\ , \qquad (11)$$

where

$$P_n(\eta)=\frac{1}{2\pi}\int_{-\infty}^{\infty}d\lambda\, e^{-i\lambda\eta}\varphi_n(\lambda)\ , \qquad (12)$$

and the characteristic function $\varphi_n(\lambda)$ is defined as

$$\varphi_n(\lambda)=\mathrm{Tr}_{\mathrm{ph}}(\rho_{\mathrm{ph}}e^{i\lambda\theta_n})\ . \qquad (13)$$

Under uniaxial strain, it is assumed that each lattice site stores the strain deformation energy s^A or s^B, according to whether an A atom or B atom is located at that site, so the infinite range of the integral Eq. (11) permits it to be rewritten

$$\langle f(\theta_n+s_n)\rangle_p=\int_{-\infty}^{\infty}d\eta\, f(\eta)P_n(\eta-s_n)\ . \qquad (14)$$

Following the procedure developed by CWS,[2] the distribution function becomes

$$P_n(\eta-s_n)=(2\pi\alpha_n)^{-1/2}e^{-(\eta-s_n)^2/2\alpha_n}\ , \qquad (15)$$

where α_n, related to the Debye-Waller factor, is roughly estimated[1] at high temperature to be

$$\alpha_n\approx 0.2T/T_m\ , \qquad (16)$$

and T_m is the melting point for pure crystals consisting of the type of atom located at the mth site. The derivation of Eq. (16) assumes that the Fermi level is at the center of the band. From Eq. (15), the strain can be seen to shift the center of the distribution function while the temperature broadens it. Consequently, the higher the temperature the less important a given strain is to the electronic properties.

The scalar integral equation for Σ now becomes

$$\int d\eta\left\langle(2\pi\alpha_n)^{-1/2}e^{-(\eta-s_n)^2/2\alpha_n}\left(\frac{\epsilon_n+\eta-\Sigma}{1-(\epsilon_n+\eta-\Sigma)F}\right)\right\rangle_c=0\ . \qquad (17)$$

Define a local distribution $P_A(\eta)$, which is the average of $P_n(\eta)$ over all configurations with an A atom at the nth site, and define $P_B(\eta)$ similarly. Then Eq. (17) becomes

$$\int d\eta\left(xP_A(\eta-s^A)\frac{\epsilon^A+\eta-\Sigma}{1-(\epsilon^A+\eta-\Sigma)F}\right.$$
$$\left.+yP_B(\eta-s^B)\frac{\epsilon^B+\eta-\Sigma}{1-(\epsilon^B+\eta-\Sigma)F}\right)=0\ . \qquad (18)$$

Again following CWS, we take

$$P_{A,B}(\eta-s^{A,B})=(2\pi\alpha_{A,B})^{1/2}e^{-(\eta-s^{A,B})^2/2\alpha_{A,B}}\ . \qquad (19)$$

The input parameters α_A and α_B are linear in temperature at high temperatures. At low temperatures the α's are proportional to T^3, rather than the Bloch T^5 behavior arising because momentum scattering rates enter for pure crystals.[5-7] We speculate that since impurity scattering, for moderately large scattering strengths δ and impurity concentrations x, broadens the electronic momentum states to widths that exceed the Debye energy, all electron-phonon scattering events correspond to large-angle scattering so the T^3 law may be the correct low-temperature limit.

IV. MODEL CALCULATIONS

In order to calculate the density of states $\rho(E)$ and the conductivity σ, we must first review the procedure for finding the self-energy Σ. Once the self-energy is obtained the density of states $\rho(E)$ can be computed. However, since in this paper we are investigating only the general trends introduced by strain, it is neither convenient nor profitable to start the calculation from a detailed $\epsilon(\vec{k})$. Instead, a simple model form for the pure crystal density of states $\rho_0(E)$ will be used. Following Velicky[3] and CWS,[2] we have adopted the Hubbard[8] ellipse model

$$\rho_0(E)=\begin{cases}(2/\pi)(1-E^2)^{1/2}\ , & |E|\le 1\ ,\\ 0 & ,\ |E|\ge 1\ ,\end{cases} \tag{20}$$

where the energy is in units of the half-bandwidth w. Define the origin of the energy and the scattering strength δ by

$$\epsilon^A=\tfrac{1}{2}\delta\ ,\quad \epsilon^B=-\tfrac{1}{2}\delta \tag{21}$$

in units of the half-bandwidth.

To solve for Σ from the integral equation, Eq. (18) or Eq. (6), rewrite it in a form that is useful for iteration (once again see CWS for details)

$$\Sigma=z-\tfrac{1}{4}F-\langle\langle[z-(\epsilon_n+\theta_n+\delta_n)-\tfrac{1}{4}F]^{-1}\rangle\rangle^{-1}\ . \tag{22}$$

This relation can be reached more directly by combining S and D instead of combining $\Theta+S$ (see Appendix B), but then the insights gained from Eq. (19) are lost. Comparing Eq. (22) with Eq. (118) in Ref. 2, it is clear that if $s^A=s^B$, the self-energy and the density of states are identical to those of an alloy without strain except for a shift of the energies ϵ^A and ϵ^B by the strain potential energy s^A. In general it can be seen from the form of Eq. (22) that the effect of the strain on the self-energy is to introduce an effective scattering strength $\delta_{\text{eff}}=\delta+s^A-s^B$.

To compute the conductivity, we assume a cubic lattice, so the averaged conductivity is isotropic. Then CWS[2] were able to derive a simplified conductivity formula

$$\sigma=\sigma_0\frac{\rho^3(\epsilon_F)}{\Delta(\epsilon_F)}\left(1+\frac{6\Delta(\epsilon_F)}{\pi\rho(\epsilon_F)}\right)\ , \tag{23}$$

if the Fermi level ϵ_F is not too close to a band edge, or other singularity, and where

$$\sigma_0=\pi^2e^2\hbar v_m^2/12\Omega_c\ , \tag{24}$$

with v_m being the maximum velocity in the band. Thus the conductivity is a function of the density of states at the Fermi level. The Fermi level under uniaxial strain at each temperature can be found by solving the equation

$$c\approx 2\int_{-\infty}^{\epsilon_F}\rho(\epsilon)\,d\epsilon\ , \tag{25}$$

where c is the average number of electrons per alloy atom and is given by

$$c=xc_A+yc_B\ , \tag{26}$$

where c_A and c_B are the numbers of electrons per atom for pure A and B crystals.

V. NUMERICAL EXAMPLES

In what follows we pick some typical values of each parameter for numerical illustration of the results. In Fig. 1 the self-energy is plotted as a function of energy in units of the half-bandwidth. The alloy has a constant concentration $x=0.5$ and scattering strength $\delta=0.8$, but four different strains are chosen: the strain potential energies are $s^A=0$, 0.02δ, 0.04δ, and 0.09δ denoted, respectively, by A, B, C, D. In this figure α_A is set equal to $\alpha_A=0.0075$, which represents a temperature near room temperature for typical crys-

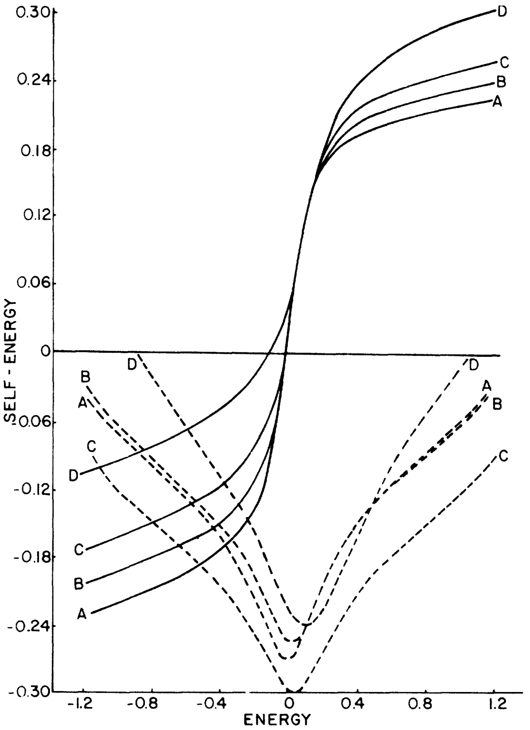

FIG. 1. Self-energies for an alloy at a finite temperature characterized by $\alpha_A=\frac{1}{2}\alpha_B=0.0075$ under four different strains: A curves, $s^A=s^B=0$; B curves, $s^A=\frac{1}{2}s^B=0.02\,\delta$; C curves, $s^A=\frac{1}{2}s^B=0.04\,\delta$; D curves, $s^A=s^B=0.09\,\delta$. The figure is for an alloy with $x=0.5$, $\delta=0.8$, and the energy is in units of half-bandwidth. The real part of the self-energy is denoted by the solid line and the imaginary part by the dashed line.

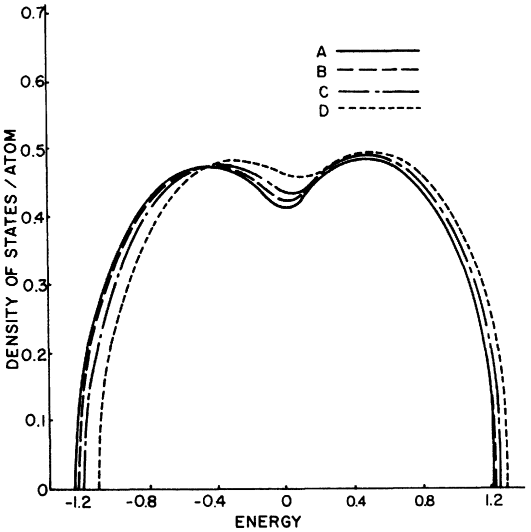

FIG. 2. Density of states under strain corresponding to the four cases in Fig. 1.

tals. The ratios α_B/α_A and s^B/s^A are both set equal to 2. The choice $\alpha_B/\alpha_A = s^B/s^A$ was made because the α's and the s's both depend on the same restoring forces so their ratios should be approximately equal. The real part of the self-energy (solid line) is shifted toward higher energies as the strain energy increases and the position of the valley in the imaginary part of self-energy has that same trend. The depth of the valley in the ImΣ decreases as s^A increases. This is a reflection of the decrease in $\delta_{\text{eff}} = \delta + s^A - s^B = \delta - s^A$ as s^A increases. The tilt of the ImΣ from high to low energy is a consequence of the choice $\alpha_B/\alpha_A = 2$. The iteration procedure yields unreliable results for ImΣ near singularities, i.e., band edges. However, in these regions ImΣ is small so the density of states can be found from the relation $\rho(E) \cong \rho_0(E - \text{Re}\Sigma(E))$.[9]

The densities of states for the strain energies corresponding to the alloy of Fig. 1 are shown in Fig. 2. Increasing the strain energy contracts the band slightly and shifts it to the right. The density of states also becomes more unsymmetric, with the upper-energy part contracted more than the lower-energy part.

Once the density of states and the imaginary part of the self-energy are known, the conductivity as a function of the Fermi level is easily obtained from Eq. (25). Figure 3 depicts the conductivity for an alloy with the same parameters as shown in Figs. 1 and 2. The small change in the temperature variation of the conductivity under strain is a result of a competition between distortions of the density of states and a shift in the Fermi level. The strain distorts the density of states which affects the conductivity by changing the effective carrier concentration and the density of final states into which electrons can scatter. However, as the density of states distorts, the Fermi level also changes in such a way that it tends to fall on the density of states of the undistorted crystal.

As discussed in previous papers practical calculations of the conductivity of an alloy are most easily pursued as a function of the number of electrons per atom instead of fixing the Fermi level. In Fig. 4 we present this kind of plot for different temperatures. The three curves correspond to the temperatures: $\alpha_A = 0.00375$, 0.0075, 0.015. Overall the change in conductivity is proportional to the strain potential energy. It is clear from the analytical expression [Eqs. (15), (19)] as well as the numerical results that the sensitivity of the conductivity to strain decreases as the temperature increases. This can be seen by comparing the spacing between two adjacent curves at each temperature. The explanation of this phenomena is that the thermal motion averages out the coherent strain displacements.

Figure 5 shows the corresponding resistivity as a function of strain potential energy s^A at various temperatures for the two cases: (a) the number of electrons per atom per spin is 0.25, (b) the number of electrons per atom per spin is 0.5. It is interesting to see that in case (b) the strain affects the resistivity much more than in case (a). This indicates that the strain effect on the electrical resistivity is sensitive to the location of the Fermi level.

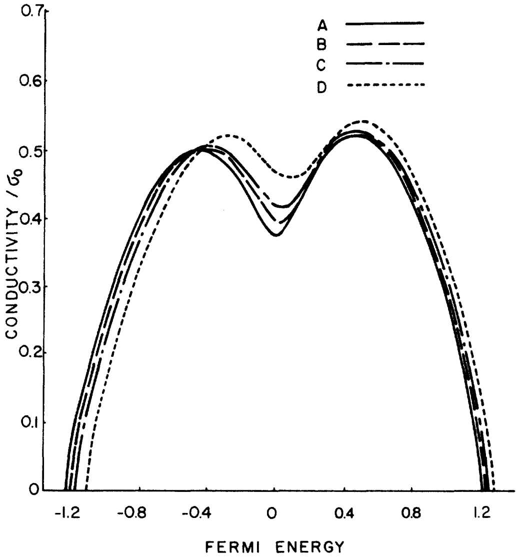

FIG. 3. Electrical conductivity σ as a function of Fermi energy under the different strains corresponding to the four cases in Fig. 1.

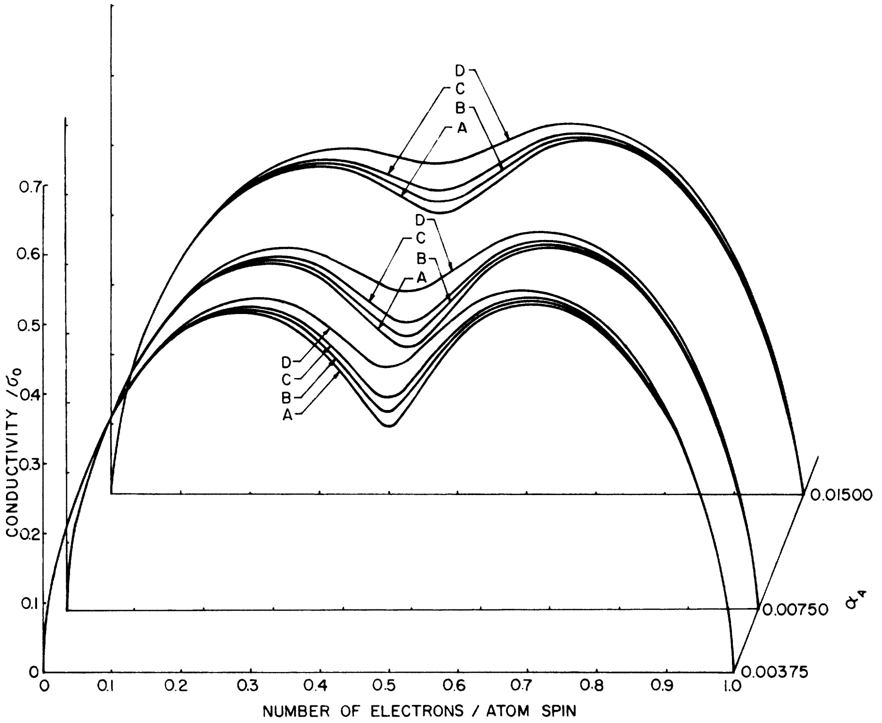

FIG. 4. Electrical conductivity as a function of the numbers of electrons per atom per spin for the alloy with $x = 0.5$, $\delta = 0.8$, and $\alpha_B/\alpha_A = s^B/s^A = 2$ under four different strains: *A* curves $s^A = 0$; *B* curves $s^A = 0.02\,\delta$; *C* curves $s^A = 0.04\,\delta$; *D* curves $s^A = 0.09\,\delta$. The three sets of curves represent the alloy at three different temperatures characterized by (a) $\alpha_A = 0.00375$, (b) $\alpha_A = 0.0075$, (c) $\alpha_A = 0.015$.

VI. CONCLUSIONS

In these concluding remarks we wish to address three questions: (a) How can the analysis presented here be used to help extract information about alloys from experimental data? (b) What direction do the insights gained from this study suggest to those concerned about technological applications of alloys, e.g., strain gauges? (c) What additions need to be made to the theory so it can be expected to apply to interesting classes of materials?

The major effect of strain on the conductivity is that it introduces an effective scattering strength $\delta_{\mathrm{eff}} = \delta + s^A - s^B \equiv \delta + \bar{s}$. Thus straining the crystal modulates the scattering strength, and for a given alloy it permits a study of the variation of the conductivity as a function of δ. Note that while all the numerical examples are for $s^A > s^B$ (given $\epsilon^A > \epsilon^B$) there is no *a priori* reason to expect this inequality to be true for all alloys. Thus the strain can cause δ_{eff} to increase or decrease depending on details of the alloy constituents' atomic properties. The kind of information that can be learned from varying the strain and the temperature can be seen most easily by examining the analytic expressions found by CWS for ρ, Δ and σ in the special case of a 50-50 alloy with $\delta < 1$, $\alpha_A = \alpha_B = \alpha$, and $\epsilon_F = 0$. (See their Appendix G.) These results are summarized in the expressions

$$\sigma(\delta_{\mathrm{eff}}, \alpha) = \sigma(\delta_{\mathrm{eff}}, 0)\left(1 + \frac{\partial \ln\sigma(\delta_{\mathrm{eff}}, 0)}{\partial \alpha}\,\alpha\right) , \qquad (27)$$

$$\sigma(\delta_{\mathrm{eff}}, 0) = \frac{16\sigma_0}{\pi^3}\left(\frac{(1-\delta_{\mathrm{eff}}^2)^2}{\delta_{\mathrm{eff}}^2} + \tfrac{3}{2}\,\pi(1-\delta_{\mathrm{eff}}^2)\right) , \qquad (28)$$

$$\frac{\partial \ln\sigma(\delta_{\mathrm{eff}}, 0)}{\partial \alpha} = \frac{8(\delta_{\mathrm{eff}}^2 - \frac{1}{4})[1 + (1-\delta_{\mathrm{eff}}^2)^2]}{\delta_{\mathrm{eff}}^2(1 + \frac{1}{2}\,\delta_{\mathrm{eff}}^2)(1-\delta_{\mathrm{eff}}^2)} , \qquad (29)$$

where it is understood that all quantities are evaluated at the Fermi energy. Since the α and strain energy variation of σ is seen from our numerical examples to be nearly linear even for the rela-

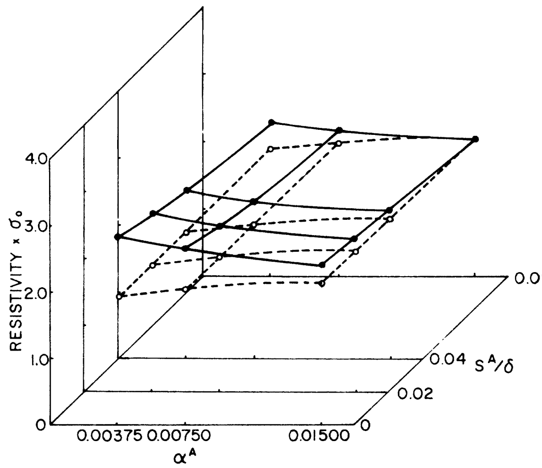

FIG. 5. Electrical resistivity at various temperatures as a function of strain potential energy per unit cell corresponding to the two cases: (a) the number of electrons/(atom spin) = 0.25 (open circles), (b) the number of electrons/(atom spin) = 0.5 (closed circles).

tively large values of $\tilde{s}$ used, a good approximation to Eq. (27) is

$$\sigma(\delta_{\mathrm{eff}}, \alpha) \cong \sigma(\delta, 0)\left\{1 + \frac{\partial \ln\sigma(\delta, 0)}{\partial\delta}\tilde{s} + \left[\frac{\partial \ln\sigma(\delta, 0)}{\partial\alpha} + \left(\frac{\partial \ln\sigma(\delta, 0)}{\partial\delta}\,\frac{\partial \ln\sigma(\delta, 0)}{\partial\alpha} + \frac{\partial^2 \ln\sigma(\delta, 0)}{\partial\alpha\partial\delta}\right)\tilde{s}\right]\alpha\right\} . \tag{30}$$

The strain energy $\tilde{s}$ is proportional to the stress (see Appendix A), and at high temperatures α is proportional to T. Thus there are four measurable quantities in Eq. (30): the conductivity at zero strain and temperature, $\sigma(\delta, 0)$; the slope of the conductivity variation with the stress P at zero temperature, $\sigma(\delta,0)[\partial \ln\sigma(\delta,0)/\partial\delta](\tilde{s}/P)$; the variation of the conductivity with temperature at zero stress, $\sigma(\delta,0)[\partial \ln\sigma(\delta,0)/\partial\alpha](\alpha/T)$; and finally the change in the last quantity with stress

$$\sigma(\delta, 0)\left(\frac{\partial \ln\sigma(\delta, 0)}{\partial\delta}\,\frac{\partial \ln\sigma(\delta, 0)}{\partial\alpha} + \frac{\partial^2 \ln\sigma(\delta, 0)}{\partial\alpha\partial\delta}\right)\frac{\tilde{s}}{P}\,\frac{\alpha}{T} .$$

There are also four unknowns in these expressions. They are δ, σ (or v_m), $\tilde{s}/P$, and α/T. Since there are four measured numbers, in principle all the unknowns can be determined. For example, the ratio of the measurable quantities

$$\left\{\left[\sigma(\delta, 0)\left(\frac{\partial \ln\sigma(\delta, 0)}{\partial\delta}\,\frac{\partial \ln\sigma(\delta, 0)}{\partial\alpha} + \frac{\partial^2 \ln\sigma(\delta, 0)}{\partial\alpha\partial\delta}\right)\frac{\tilde{s}}{P}\,\frac{\alpha}{T}\right]\left(\sigma(\delta, 0)\,\frac{\partial \ln\sigma(\delta, 0)}{\partial\alpha}\,\frac{\alpha}{T}\right)^{-1}\right\}\Big/ \left(\sigma(\delta, 0)\,\frac{\tilde{s}}{P}\,\frac{\partial \ln\sigma(\delta, 0)}{\partial\delta}\right)[\sigma(\delta, 0)]^{-1} = 1 + \left(\frac{\partial^2 \ln\sigma}{\partial\alpha\,\partial\delta}\Big/\frac{\partial \ln\sigma(\delta, 0)}{\partial\delta}\,\frac{\partial \ln\sigma(\delta, 0)}{\partial\alpha}\right) \tag{31}$$

depends only on δ as can be seen from Eqs. (27)–(29). While Eqs. (27)–(29) are valid only for a 50-50 alloy Eqs. (30) and (31) are correct, in general, but they would have to be evaluated numerically in other cases. Thus for alloy systems where the approximations of this theory hold, the combination of the temperature and strain variation of the resistivity will yield the scattering strength, the maximum electron velocity in the band, and the temperature and strain coupling constants (α/T, $\tilde{s}/P$). Once these parameters are determined then the density of states, the electron scattering rate, and other interesting quantities can be calculated for comparison against other experiments. While this analysis is correct within the context of the model treated, and it may even be useful to experimenters in the interpretation of trends in their results, the approximations are such that its detailed application should be approached with some caution. These questions will be discussed in more detail presently.

The sensitivity of strain gauges[10] is measured by the gauge factor G which is the fractional change in resistance divided by the fractional change in length l of a resistor

$$G \equiv \left(\frac{\Delta R}{R}\right)\Big/\left(\frac{\Delta l}{l}\right) = 1 + 2\eta - \frac{\partial \ln\sigma}{\partial \ln l} , \tag{32}$$

where η is Poisson's ratio which for typical materials varies from $\eta = 0.25 \rightarrow 0.5$. A Poisson ratio of 0.5 corresponds to an incompressible solid, one for which the length and width change in such a way that the volume does not vary with applied stress. Materials near their melting point seem to have Poisson ratios near 0.5. Hard materials, e.g., refractory metals near room temperature, have η values typically near 0.3.

Materials are chosen for gauges[10] that have essentially temperature-independent gauge factors because a temperature variation of the resistance will mask a strain variation. Although techniques involving several gauges in bridge arrangements exist to separate strain from temperature variations of the resistance, the ultimate limit to the sensitivity of gauges in many applications remains those caused by temperature changes. Thus, to optimize gauge performance one wants $[\partial\sigma(\delta,0)/\partial\delta]\tilde{s}$ large and negative, and $\partial \ln\sigma(\delta,0)/\partial\alpha \cong 0$. Using the general theory one can hunt through δ and x parameter space to find the best values, and then try to find a material that behaves in the prescribed fashion. In the special case of the 50-50 alloy no one choice satisfies both requirements. From Eq. (29) it is clear that $\delta = 0.5$ yields $\partial \ln\sigma(\delta,0)/\partial\alpha = 0$ so with this choice there is no first order temperature variation of the gauge factor. From Eq. (28) it is easy to show that

$$\frac{\partial \ln\sigma(\delta_{\mathrm{eff}}, 0)}{\partial \ln l} = \frac{\partial \ln\sigma(\delta)}{\partial\delta}\,\frac{\partial\tilde{s}}{\partial \ln l} = -2\delta\left(1 + \frac{\frac{3}{2}\pi\delta^4 + 2(1-\delta^2)}{(1-\delta^2)^2 + \frac{3}{2}\pi\delta^2(1-\delta^2)}\right)\frac{\partial\tilde{s}}{\partial \ln l} , \tag{33}$$

or, for $\delta = 0.5$,

$$\frac{\partial \ln\sigma(\delta_{\mathrm{eff}}, 0)}{\partial \ln l} = -2.0\,\frac{\partial\tilde{s}}{\partial \ln l} . \tag{34}$$

From Appendix A an estimate of $\partial\tilde{s}/\partial \ln l$ is

$$\frac{\partial\tilde{s}}{\partial \ln l} \approx \frac{2}{3}\left[\left(\frac{\epsilon_F^A + w}{w}\right)(1 + \eta^A) - \left(\frac{\epsilon_F^B + w}{w}\right)(1 + \eta^B)\right] \approx (0 \rightarrow 0.5) , \tag{35}$$

with the variation depending mostly on the location of the Fermi level and how close ϵ_F^A and ϵ_F^B are to one another. So for $\delta = 0.5$, $\eta = 0.3$, and $\partial\bar{s}/\partial \ln l = 0.2$ we find

$$G \cong 2.0 ,$$

a fairly typical value for gauge materials. From this estimate it is fairly clear that while $\delta = 0.5$ minimized the temperature variation of the gauge factor it may not enhance it much relative to geometric dominated gauge factors.

On the other hand as $\delta \rightarrow 1$ it is evident from Eqs. (32), (33) that the gauge factor can become large. However, in that case from Eq. (29) it can be seen that the temperature coefficient will also be quite large. We have not attempted a thorough search though the parameters δ and x to optimize the signal to error ratio for a strain gauge, but this kind of detailed analysis may be worthwhile based on the improved theory described below. However, the general trend is that small temperature and strain variations of the resistivity occur when the Fermi energy lies in regions where the impurity scattering rates Δ are large enough so the electrons are quasilocalized. Large variations with temperature and strain occur when the Fermi energy falls near band edges, or between two bands as they begin to split, where the scattering rates are small but so is the density of states, hence both are influenced by small changes.

The problem with this single band model is that alloys to which it might be expected to apply, e.g., noble metal alloys, do not have large enough scattering strengths ($\delta < 0.5$) to correspond to the interesting cases. The transition metal alloys, which do exhibit large scattering strengths, are not well represented by a one-band model. Thus, while the theory developed in this work is a necessary first step, it must be generalized, following the work of Brouers and Brauwers,[4] to a two-band model to be compared against experiment. In addition the effects caused by random transfer integrals need to be incorporated into the formalism.[11,12] Once these two first-order corrections are made, the theory should be realistic enough to predict the major trends of experiments, though to be sure, many secondary effects, e.g., scattering from magnetic clouds, impurity clusters, etc., will have to be included to complete the treatment.

APPENDIX A

For a pure metal the deformation energy per atom s can be approximated by[13]

$$s = -\tfrac{2}{3}(\epsilon_F + w)\Delta , \tag{A1}$$

where $(\epsilon_F + w)$ is the Fermi energy relative to the bottom of the band, Δ is the dilation of the crystal

$$\Delta = \Delta V/V \cong e_{xx}(1+2\eta) = c_{11}P(1+2\eta) , \tag{A2}$$

η is Poisson's ratio, c_{11} is an elastic stiffness coefficient, and e_{xx} is the strain in the x direction resulting from a stress P in the x direction. For an alloy Poisson's ratio η and the stiffness coefficients are dependent on the ion configuration around each site. However, the configuration averages can be found for these quantities so dilations Δ^A and Δ^B can be assigned depending on which type of atom occupies a given site. Thus it is possible to write

$$S^n = \mathcal{K}^n P , \quad n = A, B , \tag{A3}$$

where

$$\mathcal{K}^n = -\tfrac{2}{3}(\epsilon_F^n + w)c_{11}^n(1+2\eta^n) . \tag{A4}$$

Hence, the strain potential energies s^A and s^B are directly proportional to the stress or the strain.

To estimate the relative size of s_n and δ examine some typical parameters,[5] $e_{xx} = -10^{-2}$, $\eta = 0.3$, $\epsilon_F + w = 10\ \text{eV} = 1.6\times10^{-11}$ erg, $\delta = 5\ \text{eV} = 8\times10^{-12}$ erg, then $s^A \simeq 0.02\delta$. The numerical results displayed in the figures are for strain deformation energies around the typical value arrived at here.

APPENDIX B

The average shown in Eq. (22) can be reached in a more straightforward way by combining S and D in the simple band model Eq. (1). Let

$$\begin{aligned} D' = D + S &= \sum_n |n\rangle(\epsilon_n + s_n)\langle n| \\ &= \sum_n |n\rangle\epsilon_n'\langle n| , \end{aligned} \tag{B1}$$

where

$$\epsilon_n' = \epsilon_n + s_n , \tag{B2}$$

so the strain only changes the scattering strength. Following the procedures in CWS's paper, Eq. (40) is reached by substituting

$$\begin{aligned} \epsilon^{A'} &= \epsilon^A + s^A , \\ \epsilon^{B'} &= \epsilon_B + s^B . \end{aligned} \tag{B3}$$

---

*Work supported in part by NASA grants Nos. NASA-NSG-1034 and NASA-NGL-006-055.

[1] B. Velicky, S. Kirkpatrick, and H. Ehrenreich, Phys. Rev. 175, 747 (1968).

[2] A. B. Chen, G. Weisz, and A. Sher, Phys. Rev. B 5, 2897 (1972).

[3] B. Velicky, Phys. Rev. 184, 614 (1969).

[4] F. Brouers and M. Brauwers, J. Phys. (Paris) 36, L17 (1975).

[5] C. Kittel, *Introduction to Solid Physics*, 3rd Ed. (Wiley, New York, 1966), p. 117.

[6] S. F. Edwards, Philos. Mag. 3, 1020 (1958).

[7] J. L. Beeby, Phys. Rev. 135, A130 (1964).

[8] J. Hubbard, Proc. R. Soc. Lond. A 281, 401 (1964).

[9] Equation (130) in Ref. 2 in the limit $\mathrm{Im}\Sigma \to 0$.

[10] M. Dean, III, and R. D. Douglas, *Semiconductor and Conventional Strain Gages* (Academic, New York, 1962).

[11] H. Fukuyama, H. Krakauer, and L. Schwartz, Phys. Rev. B 10, 1173 (1974).

[12] H.-C. Hwang and A. Sher, Phys. Rev. B 12, 5514(1975).

[13] J. M. Ziman, *Principles of the Theory of Solids* (Cambridge University, Cambridge, 1964), p. 177, Eq. (6.93).